International Journal of Mass Spectrometry 309 (2012) 200–205

Contents lists available at SciVerse ScienceDirect

International Journal of Mass Spectrometry

journal homepage: www.elsevier.com/locate/ijms

Diagnosis of lung cancer based on direct-infusion electrospray mass spectrometry of blood plasma metabolites

Petr G. Lokhov*, Oleg N. Kharybin, Alexander I. Archakov

Institute of Biomedical Chemistry RAMS, 119121, Pogodinskaya st., 10, Moscow, Russia

ARTICLE INFO

Article history:
Received 15 September 2011
Received in revised form 5 October 2011
Accepted 6 October 2011
Available online 17 October 2011

Keywords:
Direct-infusion mass spectrometry
Lung cancer
Electrospray ionization
Blood plasma metabolites
Diagnostics

ABSTRACT

Lung cancer is one of the most prevalent types of cancer in men and women, and is a leading cause of cancer-related death. Early detection of lung cancer may profoundly reduce cancer death rates. It is therefore extremely important to develop laboratory tests to detect human lung cancer, including at clinically asymptomatic stages. To this end, mass spectrometric metabolite analysis was performed on blood samples collected from patients with lung cancer ($N = 100$) and age-matched controls ($N = 100$). Proteins were extracted from blood plasma with methanol, and the remaining metabolite fractions were directly analyzed using electrospray ionization (ESI) mass spectrometry. Mass spectra obtained were converted into binary format, aligned, reduced to several variables by principal component analysis (PCA), and finally, classified as cancer cases versus controls by a support vector machine (SVM) algorithm. Repeated random sub-sampling validation revealed an accuracy of classification as high as 93.3% (sensitivity 94.1%, selectivity 92.4%), strongly indicating that direct-infusion ESI mass spectrometry of blood plasma metabolites offers great clinical potential in the diagnosis of early-stage human lung cancer.

1. Introduction

Despite extensive research and clinical efforts to prevent and manage lung cancer, it remains the leading cause of deaths from cancer for both men and women. Furthermore, lung cancer is responsible for the deaths of ~1.3 million people worldwide every year, and this number is more than that for breast, prostate, colon, and pancreatic cancers combined [1,2]. More alarmingly, most lung cancers are diagnosed in a late, symptomatic stage, thereby resulting in very unfavorable outlook. Five-year survival of patients with lung cancer has not changed for last 15–20 years and is about 15% in the USA and other developed countries [1].

Imaging radiology techniques are currently widely used to detect cancerous lesions in the lung at the early stage. Unfortunately, however, the control trials have shown that their application do not decrease mortality from lung cancer [3]. Moreover, treatment options for the later stages of lung cancer are rarely curative [4–9]. Correspondingly, it is extremely important that diagnostic markers for lung cancer in its early, asymptomatic stages be identified. The tumor markers currently available for detecting lung cancer are characterized by insufficient sensitivity. For example, the Hamburger Group for the Standardization of Tumor Markers has reported a sensitivity of 58.0%, 66.4%, and 58.6% for carcinoembryonic antigen (CEA), cytokeratin 19 fragments (CYFRA), and neuron specific enolase (NSE), respectively [10,11]. It is suggested that the identification of markers associated with higher sensitivities would have a profound impact on the rate of death from lung cancer.

In metabolomics, a large number of metabolites can be detected from samples and, in the case of bodily fluids, this capacity offers a great potential for diagnostics. Correspondingly, recent developments in metabolomics have showed promise in the metabolite-based detection of cancer. The majority of metabolomic studies on cancer, including those for lung cancer, have been conducted using multi-stage protocols involving magnetic resonance spectroscopy and mass spectrometry [12–18], including metabolic study of blood plasma [14,19–21]. As a result, numerous metabolites have been identified, some of which are related to lung cancer [17,18].

Among metabolomics technologies, direct-infusion mass spectrometry seems most suitable in developing a prototype for clinical analysis. There are several examples in which direct mass spectrometry has been successfully used [15,16,22–27]. Results of these studies have shown that the major advantage of direct mass spectrometry is the high reproducibility of results. Due to this reproducibility, subsequent effective classification of metabolite mass spectra has been possible [28]. Direct-infusion mass spectrometry implies direct infusion of an analyzed biological material to the ionization source of the mass spectrometer, without any preliminary separation. This technique can be used for single-step

* Corresponding author. Tel.: +7 903 7445171; fax: +7 495 2450857.
E-mail address: lokhovpg@rambler.ru (P.G. Lokhov).

1387-3806/$ – see front matter © 2011 Elsevier B.V. All rights reserved.
doi:10.1016/j.ijms.2011.10.002

Table 1
Clinical characteristics of control subjects and lung cancer patients.

Characteristic	Control subjects (plasma)	Lung cancer patients (plasma)
N (male/female)	100 (89/11)	100 (88/12)
Age (median/range)	59/37–71	60/44–76
Smokers/non-smokers	77/23	93/7
Pathological diagnosis (Sq/SCLC/Ad/LCC/Mx/NOS)[a]	–	58/7/12/4/9/10
Cancer stages (I/II/III/IV)	–	24/12/50/14

Sq, squamous cell carcinoma; SCLC, small cell lung carcinoma; Ad, adenocarcinoma; LCC, large cell carcinoma; Mx, Mixed carcinoma; NOS, carcinoma non specified. Cancer stages were based on the TNM classification.

[a] Classification is according to International Classification of Diseases for Oncology.[40]

rapid readily reproducible analysis of metabolites, which may serve as a prototype for clinical analyses. Therefore in this study, direct-infusion electrospray ionization (ESI) mass spectrometry of blood plasma metabolites was studied as a prototype for the diagnosis of lung cancer.

2. Materials and methods

2.1. Study design and subjects

The study is based on the epidemiological case–control study of lung cancer carried out in Department of epidemiology and prevention of Russian N.N. Blokhin Cancer Research Center. Cases were recruited from Russian N.N. Blokhin Cancer Research Center (Moscow) and Moscow Cancer Dispensary. The study was approved by relevant ethical review committee, and participants gave written informed consent. Cases were patients with newly diagnosed lung cancer. Controls were recruited from the neighboring general hospitals in Moscow with the same catchment areas as for cases. Controls were selected from a broad range of diagnostic categories excluding malignant neoplasm and diseases considered to be unrelated to tobacco smoking. The data on demographic characteristics, education, life-style habits, occupational, family and medical history of cases and controls were collected by specially trained interviewers administering a standard questionnaire. Fifty-eight lung cancer patients were histologically diagnosed as having squamous cell carcinoma, 12 with adenocarcinoma, 7 with small cell, 4 with large cell, 9 with mixed carcinoma, and 10 with carcinoma non-specified (Table 1). The stage distribution of cancer patients was as follows: stage I, $N = 24$: stage II, $N = 12$; stage III, $N = 50$; and stage IV, $N = 14$ patients. The age ranges of controls and lung cancer patients were 37–71 years (median 59) and 44–76 (median 60), respectively. Current smokers constituted a larger portion of the case group (93%) than the control group (77%).

Blood samples for metabolomic analysis were obtained both from cases and controls within 2–3 days after admition to the clinic and before the start of any treatment. Blood was taken from the cubital vein before the morning meal; blood samples (3 ml) were placed into glass tubes containing K_2EDTA (BD Vacutainer, USA) and centrifuged within 15 min after blood collection at $1600 \times g$ and room temperature. Resultant blood plasma was then subdivided into four equal aliquots that were pipetted into plastic tubes. These tubes were marked and frozen at −80 °C. The frozen blood samples were transported in special thermo containers and kept until analysis at −80 °C. The analyzed samples were subjected to one freeze/thaw cycle.

For the plasma deproteinization, aliquots (100 μl) were mixed with 100 μl of water (LiChrosolv, Merck, USA) and 800 μl of methanol (Fluka, Germany) and incubated at −20 °C for 10 min. After centrifugation at $13{,}000 \times g$ (Eppendorf MiniSpin plus centrifuge, Germany) for 10 min, the deproteinized supernatant was transferred into clean plastic Eppendorf tubes. Solvent was evaporated at 45 °C for 3 h using a vacuum SpeedVac evaporator (Eppendorf). A dry residue was dissolved in 100 μl of 95% acetonitrile (Acros Organics, USA) with addition of 0.1% formic acid (Fluka). Samples were then sonicated using a Bandelin RM 40UH washer (Sonorex Technik, Germany) 5 times for 30 s for better solubilization of the residue. Samples were then centrifuged at $13{,}000 \times g$ for 10 min and the resultant supernatant was used for mass spectrometry analysis.

2.2. Direct-infusion mass spectrometry

Mass spectrometry analysis was performed using a MicrOTOF-Q hybrid quadrupole time-of-flight mass spectrometer (Bruker Daltonics, Germany) equipped with an electrospray source of ionization. The mass spectrometer was set up to priority detection of ions with the range from m/z 50 to 1000 at a mass accuracy of 2–4 ppm. Spectra were recorded in the mode of detection of both positive and negative ion charge. Samples were injected into the electrospray ionization source with a glass syringe (Hamilton Bonaduz, Switzerland) connected to a syringe injection pump (KD Scientific, USA). The flow rate of samples to the ionization source was 180 μl/h, and samples were injected in a randomized order (e.g., control samples were run in between case samples). Mass spectrometry analysis of all samples was performed over the course of a month (with 10 samples completed/working day). Mass spectra were obtained in the DataAnalysis program 3.4 (Bruker Daltonics) by summarizing 5 min signals.

2.3. Mass spectra processing

Using the DataAnalysis program masses of ion metabolites were determined from peaks in mass spectra. All peaks above noise level were selected. Two peaks were considered to be related to the same metabolite if their mass difference did not exceed 0.01 Da. Resultant lists of masses of positively charged metabolite ions were pooled, binned in intervals of 0.01 Da and were coded into the binary format, where 'one' is the presence of a measured metabolite mass in an interval, 'zero' is the absence of this metabolite [15]. Resulted binary matrix of mass spectrometry data was used for further analysis. Mass spectra processing was performed using a Matlab v.12 program (Mathworks, USA).

2.4. Binary matrix alignment

Binary matrix data were aligned according to the algorithm presented in Fig. 1. Briefly, negatively correlated neighboring lines in binary matrices were combined. This action was repeated several times with stepwise reduction of the correlation coefficient used to select neighboring negatively correlating lines. The result of the alignment is shown in Fig. 2. Binary matrix alignment was done using Matlab software. After alignment, uninformative lines in binary matrices, which contained >80% zeros, were removed.

2.5. Correction of ionic inconsistency in blood plasma samples

Measured ion masses in combination with isotope patterns were used to identify the peak of the K_2Cl^+ ion in mass spectra. All metabolite ions with peak intensities correlating (correlation coefficient >0.15 or <−0.15) with the intensity of this peak, were excluded from our analysis.

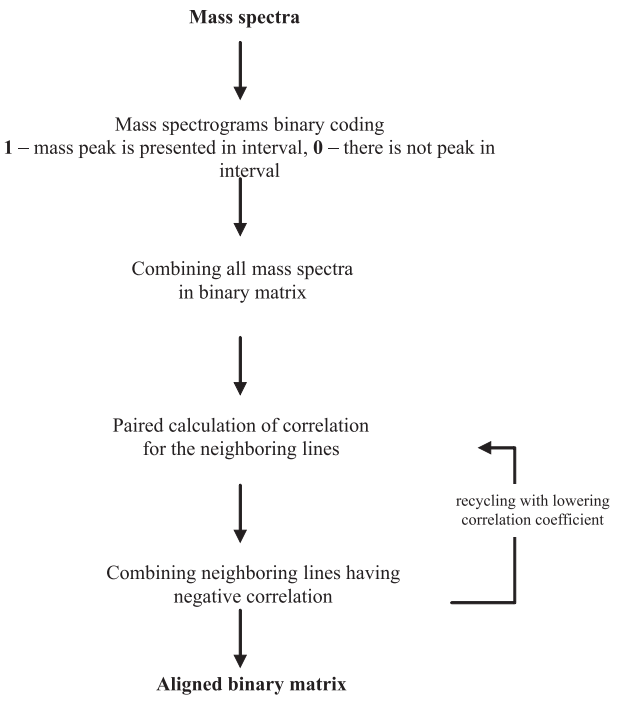

Fig. 1. Algorithm of binary-coded mass spectra alignment. Realization of the given algorithm was carried out using Matlab program. Algorithm results are presented in Fig. 2.

2.6. Dimensionality reduction of mass spectrometry data

Binary matrix data were processed by principal component analysis (PCA) using the *princomp* function of the Matlab program. Projections of binary matrix columns (corresponding to plasma samples) on the first seven principal components, were further used for sample classification.

2.7. Blood plasma samples classification

Blood plasma samples were classified by means of the support vector machine (SVM) method using a linear SVM classifier (the *svmtrain* function) from the Matlab program. Coordinates of binary-coded mass spectra projections on first seven principal components were used as the input data for classification.

The efficiency of classification was tested by the '*repeated random sub-sampling validation*' method. It consists in removal of randomly selected 10% of input data and training of the classifier using remaining data with subsequent testing of the classifier using the data, which was not included into the training set. Classification was repeated 10,000 times and classification accuracy was calculated as a mean value. The confidence interval for the accuracy of classification was calculated by the method of Vapnik for calculation of the confidence intervals proposed for the classifier with a teacher [29]. Calculations were performed for the confidence probability of 0.95.

3. Results and discussion

3.1. Mass spectrometry

Direct-infusion mass spectrometry analysis of blood plasma samples resulted in detection of approximately 1500 positively charged ions per sample. No significant changes in the number of detected ions were found between controls and lung cancer patients. A typical mass spectrum is shown in Fig. 3. Peaks in mass spectra representing metabolites with a mass-to-charge (m/z) ratio up to 500 are shown. A characteristic distribution of mass spectrometry peaks was observed in the region associated with higher m/z ratios (Fig. 3), which corresponds to the detection of high-abundance plasma lipids such as phospholipids, di and triglycerides, and lysophospholipids [16,30,31]. Correspondingly, since the area above m/z 500 was occupied by the peaks of high-abundance plasma lipids, only peaks with a m/z ratio $\leq$500 were used as a diagnostic tool in the present study. Mathematical conversion of mass spectra into the binary code yielded binary vector (i.e., metabolic bar-code, fingerprint, signature), which represented multivariable characteristics of blood plasma, where binary values indicate the presence or absence of metabolite ions in specific m/z. Such binary coding simplifies further mass spectrometry data alignment, and increases diagnostic accuracy up to 4–5% of what was empirically established in this study.

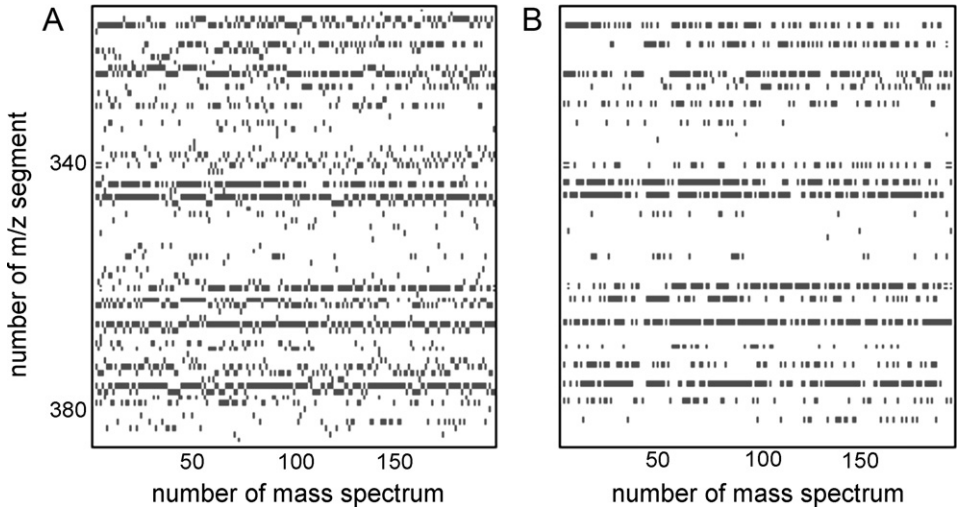

Fig. 2. Fragment of a binary matrix of mass spectrometry data before and after alignment. (A) Matrix fragment before alignment, showing that the majority of metabolite ion peaks are not adjusted with each other, and thus does not allow for statistical analysis. (B) The same fragment of a matrix after alignment, showing that the majority of metabolite ion peaks are adjusted with each other, allowing statistical analysis. The dash specifies presence of a metabolite ion peak in a specific m/z cell of a matrix.

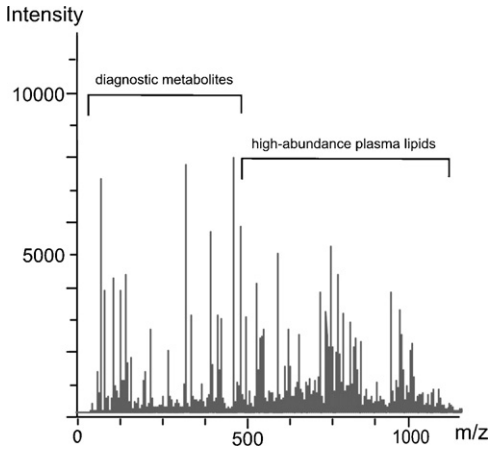

Fig. 3. Representative mass spectrum of blood plasma metabolites. Metabolite mass spectrum was obtained following the direct injection of deproteinized blood plasma sample into an electrospray ion source of a hybrid quadrupole time-of-flight mass spectrometer. Mass spectrum was obtained for positively charged metabolites. Area above m/z 500 corresponds to peaks of high-abundance plasma lipids such as phospholipids, di- and triglycerides, and lysophospholipids. Peaks with an area up to a m/z of 500 were evaluated for their potential to be diagnostic metabolites.

3.2. Mass spectrometry data alignment

As several mass spectra are processed, it is important that spectra are aligned to ensure that similar metabolite intensities are correctly matched in each sample. Without such an alignment procedure, it is possible to make errors in identifying signals from metabolites with similar molecular masses. Moreover, in the case of mass spectrometry-based diagnostics, such adjustments are necessary as alignment problems can arise when different laboratories generate mass spectra for diagnostics. In a recent study utilizing mass spectrometers located in different medical centers, Semmes et al. [32] indicated that problems with alignment are important barriers that must be overcome to ensure that data from different centers are compatible. Furthermore, Baggerly et al. [33] also identified alignment problems as a significant hindrance to achieving reproducibility with samples collected within the same laboratory.

The present study offers simple and straightforward algorithm for alignment adjustments to binary-coded mass spectra. This algorithm may be useful in standardizing measurements taken from the same instrument or from many different instruments, when locations of corresponding peaks across spectra are inconsistent. Fig. 2 shows that mass spectrometric data collected in the binary matrix, after processing, are aligned and therefore suitable for further statistical analysis.

3.3. Correction of ionic inconsistency in blood plasma samples

ESI is a soft-ionization technique used in mass spectrometry to produce ions. Ions observed by ESI-MS are quasimolecular ions created by the addition of a proton (a hydrogen ion), denoted $[M+H]^+$, or another cation, such as sodium $[M+Na]^+$ or potassium $[M+K]^+$. In each case, the detected mass depends on the mass of the added ion. Therefore in the case of direct-infusion ESI-mass spectrometry, concentrations of these ions in samples should be constant, or at least within a narrow range. Table 2 summarizes ions in blood plasma samples that influence ESI mass spectra. Proton and sodium ions do not influence ESI mass spectra due to their narrow concentration ranges. Potassium levels in plasma (3.5–5.0 mM) must be very stable to avoid the dangers symptoms of metabolic shock, which begin to materialize when potassium levels exceed 5.0 mM. Simultaneously, the range of potassium levels found within human red blood cells is 80–120 mM [34], which is about 20-fold that found in blood plasma. Furthermore, it is well known that potassium leaks from cells when plasma is not immediately separated from collected blood, or when blood has been temporarily stored, or plasma is handled roughly [35,36]. Therefore, K^+ concentration ranges may vary widely across blood plasma samples, potentially disrupting ESI mass spectra.

Looking at mass spectra is a very simple way to monitor K^+ concentrations in plasma during mass spectrometry-based diagnostics. Measured ion mass in combination with isotope pattern allowed for the identification of potassium-containing ions, and the most intensive among these ions are summarized in Table 3. The ion peak corresponding to K_2Cl^+ was shown to have the highest intensity and a characteristic isotopic pattern, which is easily identified in the spectrum (Fig. 4A). Measurement of K_2Cl^+ ion intensities in spectra confirmed that plasma samples had different potassium levels (intensities were varied from 100 to 3400 units; see Fig. 4B). Therefore, it was decided that all metabolites whose intensities correlated with K^+ level should be excluded from further analysis due to the likelihood that their intensities reflect K^+ leakage from erythrocytes at sample preparation rather than providing useful diagnostic information. Such peaks were found in mass spectra by calculating correlation coefficient for intensities of all metabolite ions with intensity of K_2Cl^+ ion peak (m/z 112.896). This correction increased the final accuracy of the diagnostic system by 15–20%, indicating that a constant level of potassium ions in samples is essential for diagnostics based on direct-infusion ESI-mass spectra. Otherwise, as in our case, all ions correlating with the K_2Cl^+ ion peak should be excluded from analysis.

Table 2
Level of cations that affect ESI-mass spectra in blood plasma samples.

Ion	Level in blood plasma sample	Notation
H^+	pH ~2.8	Initial pH of blood plasma is constant and equal to 7.35–7.45. However, blood plasma samples prepared for ESI mass spectrometry are premixed with formic acid and have final pH ~2.8.
Na^+	136–145 mM	This level corresponds to physiological conditions.
K^+	3.5–60 mM	Blood plasma contains 3.5–5.0 mM of K^+ ions. Most abundant blood cells, erythrocytes, contain 80–120 mM of K^+ ions. Therefore, final concentration of K^+ ions in blood plasma samples consists of initial plasma K^+ ions and K^+ ions leaked from cells.
Other ions	–	Level of other ions is too low for influencing ESI mass spectrograms.

Table 3
The most intense potassium-containing ions identified in mass spectrum of blood plasma metabolites.

Molecular mass (Da)		Elemental composition	Isotope pattern[a] (%)	Peak intensity[b]
Measured	Calculated			
96.921	96.922	$KNaCl^+$	100, 39, 2	1506 (51.5%)
112.897	**112.896**	**K_2Cl^+**	**100, 46, 5**	**2923 (100.0%)**
170.854	170.854	$K_2NaCl_2^+$	100, 78, 20, 2	111 (3.8%)
186.825	186.828	$K_3Cl_2^+$	100, 86, 26, 3	23 (0.8%)
244.789	244.787	$K_3NaCl_3^+$	85, 100, 45,10	83 (2.8%)

Bold typed line corresponds to ion used for measuring potassium levels in blood plasma samples.

[a] 100% corresponds to the most intense peak in the isotope pattern; peaks with an intensity of less than 2% are not shown in the pattern.

[b] The most intense peak was taken as 100% and the relative peak intensities are shown in parentheses.

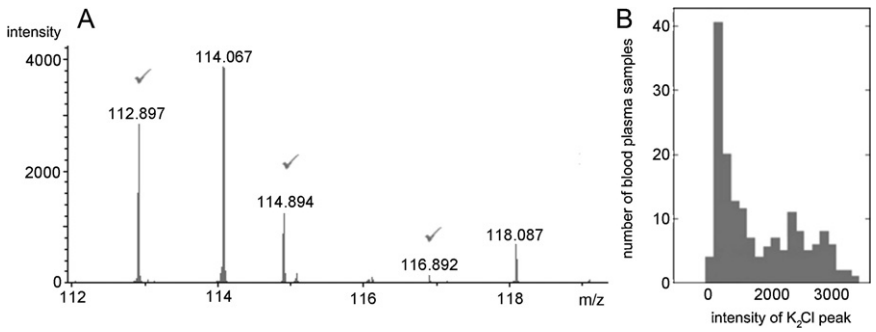

Fig. 4. Fragment of ESI mass spectrum of blood plasma metabolites showing K_2Cl^+ ions (A) and distribution of potassium levels in blood plasma samples (B). The metabolite mass spectrum was obtained by direct infusion of deproteinized blood plasma samples to an ESI device connected to a MicrOTOF-Q mass spectrometer tuned to detect positively charged ions. K_2Cl^+ ions are labeled with a '√'. The distribution of potassium levels in blood plasma samples is shown as a histogram of K_2Cl^+ peak (m/z 112.896) intensities in 200 mass spectra.

3.4. Dimensionality reduction of mass spectrometry data

As a source of data for diagnostics, mass spectrometric metabolite profiles, represent multivariable (multidimensional) characteristics of an organism consisting of hundreds of intensities (variables) of a metabolite's peaks in mass spectra. Direct application of such multivariable data leads to overfitting of any diagnostic system. Overfitting occurs when there are too many variables relative to the number of samples. A diagnostic which has been overfit will have poor predictive performance, as it can exaggerate minor fluctuations in input data. To avoid overfitting, the rule of 10–15 samples per variable should be followed. When this requirement was maintained, the dimensionality of the mass spectrometry data were reduced by PCA. Therefore, the binary matrix was replaced by their projections in the space of the seven principal components, which covered ~80% (value returned by the *princomp* function) of all variability presented in mass spectra. Thus, dimensionality reduction was performed without essential loss of data presented in mass spectra.

3.5. Sample classification

Projection of binary-coded mass spectra in space of the seven principal components allows their separation by a discriminating plane into two classes. This plane was built up by the Support Vector Machine (SVM) algorithm, which may classify multidimensional data by their separation into classes using formation of a hyperplane in a given multidimensional space. Formally, sample separation into classes is a model diagnostic system for detection of lung cancer and efficiency of this system may be determined by testing. To this end, classification efficiency was tested using '*repeated random sub-sampling validation*', and the results were used to calculate diagnostic sensitivity, specificity, and accuracy (Table 4).

Table 4
Characteristics of the mass spectrometry-based diagnostics of the lung cancer I–IV stages.

Samples set	Diagnostics characteristics (%)		
	Sensitivity	Specificity	Accuracy
I stage *vs. N*	100.0	92.4	93.9 ± 0.12[a]
II stage *vs. N*	91.4	92.4	92.3 ± 0.13
III stage *vs. N*	92.3	92.4	92.4 ± 0.11
IV stage *vs. N*	93.0	92.4	92.5 ± 0.13
I, II stages *vs. N*	97.1	92.4	93.6 ± 0.12
I–III stages *vs. N*	94.3	92.4	93.3 ± 0.10
I–IV stages *vs. N*	94.1	92.4	93.3 ± 0.10

[a] The confidence interval for reliability was calculated for the confidence probability of 0.95. *N* – the set of plasma samples corresponding to controls (*N* = 100).

Table 4 shows that high accuracy in diagnosing stages I–IV of lung cancer were obtained in this study. However, it should be noted that high efficiency of diagnosis in early-stages of the disease (for example, 100% sensitivity for stage I), most likely does not correlate with cancer progression in the organism. The small size of tumors in the early stages of cancer, as well as the absence of cellular specificity of almost all metabolites, makes detection of cancer-specific metabolites in early stages improbable. Sensitivity in detecting lung cancer in its early stages may be explained by lung cancer etiology. For example, the most common causes of lung cancer include long-term exposure to tobacco smoke [37] and air pollution [38,39]. Therefore, it is probable that early cancer diagnostics are detecting exposure, rather than markers of disease, and thus may reveal an increased risk of lung cancer. If so, blood plasma metabolite profiles would have predictive value.

4. Concluding remarks

This study demonstrated that mass spectrometry of blood plasma metabolites has great potential as a tool for diagnosing lung cancer. Diagnostic flow charts include blood plasma sampling, sample deproteinization, metabolic profiling by direct-infusion ESI-mass spectrometry, and data processing (binary coding, alignment, correction of ionic inconsistency, data dimensionality reduction, and sample classification). The correct choice at each step of the diagnostic process prevented lost information related to blood plasma metabolites, resulting in high diagnostic accuracy for lung cancer, including early-stage disease.

Acknowledgments

We express our gratitude to the volunteers who participated in this study and to the staff of the Russian N.N. Blokhin Cancer Research Center (Moscow) who contributed to the study. This work was funded by RFFI grant 09-04-12271-ofi_m.

References

[1] A. Jemal, R. Siegel, E. Ward, Y. Hao, J. Xu, T. Murray, M.J. Thun, Cancer statistics, 2008, CA. Cancer J. Clin. 58 (2008) 71.
[2] D.M. Cutler, J. Econ. Perspect. 22 (2008) 3.
[3] R. MacRedmond, P.M. Logan, M. Lee, D. Kenny, C. Foley, R.W. Costello, Thorax 59 (2004) 237.
[4] R.E. Coleman, J. Nucl. Med. 40 (1999) 814.
[5] K. Higashi, Y. Ueda, K. Ayabe, A. Sakurai, H. Seki, Y. Nambu, H. Shikata, S. Taki, H. Tonami, S. Katsuda, I. Yamamoto, Nucl. Med. Commun. 21 (2000) 707.
[6] K. Higashi, Y. Ueda, M. Yagishita, Y. Arisaka, A. Sakurai, M. Oguchi, H. Seki, Y. Nambu, H. Tonami, I. Yamamoto, J. Nucl. Med. 41 (2000) 85.
[7] R.J. Hicks, V. Kalff, M.P. MacManus, R.E. Ware, A. Hogg, A.F. McKenzie, J.P. Matthews, D.L. Ball, J. Nucl. Med. 42 (2001) 1596.
[8] J. Guo, K. Higashi, H. Yokota, Y. Nagao, Y. Ueda, Y. Kodama, M. Oguchi, S. Taki, H. Tonami, I. Yamamoto, J. Nucl. Med. 45 (2004) 1334.

[9] K. Higashi, I. Matsunari, Y. Ueda, R. Ikeda, J. Guo, M. Oguchi, H. Tonami, I. Yamamoto, Ann. Nucl. Med. 17 (2003) 1.
[10] Y. Maeda, Y. Segawa, N. Takigawa, I. Takata, N. Fujimoto, Intern. Med. 35 (1996) 764.
[11] P. Stieber, H. Dienemann, A. Schalhorn, U.M. Schmitt, J. Reinmiedl, K. Hofmann, K. Yamaguchi, Anticancer Res. 19 (1999) 2673.
[12] L.L. Cheng, M.A. Burns, J.L. Taylor, W. He, E.F. Halpern, W.S. McDougal, C.L. Wu, Cancer Res. 65 (2005) 3030.
[13] K.W. Jordan, C.B. Adkins, L. Su, E.F. Halpern, E.J. Mark, D.C. Christiani, L.L. Cheng, Lung Cancer 68 (2010) 44.
[14] G. Peng, U. Tisch, O. Adams, M. Hakim, N. Shehada, Y.Y. Broza, S. Billan, R. Abdah-Bortnyak, A. Kuten, H. Haick, Nat. Nanotechnol. 4 (2009) 669.
[15] P.G. Lokhov, M.I. Dashtiev, L.V. Bondartsov, A.V. Lisitsa, S.A. Moshkovskii, A.I. Archakov, Biomed. Khim. 55 (2009) 247.
[16] P.G. Lokhov, M.I. Dashtiev, S.A. Moshkovskii, A.I. Archakov, Metabolomics 6 (2010) 156–163.
[17] S. Hori, S. Nishiumi, K. Kobayashi, M. Shinohara, Y. Hatakeyama, Y. Kotani, N. Hatano, Y. Maniwa, W. Nishio, T. Bamba, E. Fukusaki, T. Azuma, T. Takenawa, Y. Nishimura, M. Yoshida, Lung Cancer (2011).
[18] J. Carrola, C.M. Rocha, A.S. Barros, A.M. Gil, B.J. Goodfellow, I.M. Carreira, J. Bernardo, A. Gomes, V. Sousa, L. Carvalho, I.F. Duarte, J. Proteome Res. 10 (2011) 221.
[19] G.A. Gowda, S. Zhang, H. Gu, V. Asiago, N. Shanaiah, D. Raftery, Expert Rev. Mol. Diagn. 8 (2008) 617.
[20] M. Osl, S. Dreiseitl, B. Pfeifer, K. Weinberger, H. Klocker, G. Bartsch, G. Schafer, B. Tilg, A. Graber, C. Baumgartner, Bioinformatics 24 (2008) 2908.
[21] R. Xue, Z. Lin, C. Deng, L. Dong, T. Liu, J. Wang, X. Shen, Rapid Commun. Mass Spectrom. 22 (2008) 3061.
[22] J.C. Erve, W. Demaio, R.E. Talaat, Rapid Commun. Mass Spectrom. 22 (2008) 3015.
[23] R. Goodacre, S. Vaidyanathan, G. Bianchi, D.B. Kell, Analyst 127 (2002) 1457.
[24] L. Lin, Q. Yu, X. Yan, W. Hang, J. Zheng, J. Xing, B. Huang, Analyst 135 (2010) 2970.
[25] M.J. Lerma-Garcia, G. Ramis-Ramos, J.M. Herrero-Martinez, E.F. Simo-Alfonso, Rapid Commun. Mass Spectrom. 22 (2008) 973.
[26] A. Koulman, B.A. Tapper, K. Fraser, M. Cao, G.A. Lane, S. Rasmussen, Rapid Commun. Mass Spectrom. 21 (2007) 421.
[27] G. McDougall, I. Martinussen, D. Stewart, J. Chromatogr. B: Analyt. Technol. Biomed. Life Sci. 871 (2008) 362.
[28] K. Dettmer, P.A. Aronov, B.D. Hammock, Mass Spectrom. Rev. 26 (2007) 51–78.
[29] V.N. Vapnik, Algoritmy i programmy vosstanovleniya zavisimostei, (Algorithms and Programs for Restoration of Dependencies), Nauka, Moscow, 1984.
[30] C. Wang, J. Yang, P. Gao, X. Lu, G. Xu, Rapid Commun. Mass Spectrom. 19 (2005) 2443.
[31] J. Dong, X. Cai, L. Zhao, X. Xue, L. Zou, X. Zhang, X. Liang, Metabolomics 6 (2010) 478.
[32] O.J. Semmes, Z. Feng, B.L. Adam, L.L. Banez, W.L. Bigbee, D. Campos, L.H. Cazares, D.W. Chan, W.E. Grizzle, E. Izbicka, J. Kagan, G. Malik, D. McLerran, J.W. Moul, A. Partin, P. Prasanna, J. Rosenzweig, L.J. Sokoll, S. Srivastava, I. Thompson, M.J. Welsh, N. White, M. Winget, Y. Yasui, Z. Zhang, L. Zhu, Clin. Chem. 51 (2005) 102.
[33] K.A. Baggerly, J.S. Morris, K.R. Coombes, Bioinformatics 20 (2004) 777.
[34] M. Pietrzak, M.E. Meyerhoff, Anal. Chem. 81 (2009) 5961.
[35] R. Bellevue, H. Dosik, G. Spergel, B.D. Gussoff, J. Lab. Clin. Med. 85 (1975) 660.
[36] G. Colussi, D. Cipriani, Am. J. Nephrol. 15 (1995) 450.
[37] Lung Carcinoma: Tumors of the Lungs, in: R.S. Porter (Ed.), Merck Manual Professional Edition, Online edition, Merck & Co, Inc., Whitehouse Station, N.J., U.S.A, 2008, http://www.merckmanuals.com/professional/pulmonary_disorders/tumors_of_the_lungs/lung_carcinoma.html.
[38] Z. Kabir, K. Bennett, L. Clancy, Ir. Med. J. 100 (2007) 367.
[39] Y.M. Coyle, A.T. Minahjuddin, L.S. Hynan, J.D. Minna, J. Thorac. Oncol. 1 (2006) 654.
[40] A. Fritz, A. Jack, D.M. Parkin, C. Percy, S. Shanmugarathan, L. Sobin, S. Whelan, International Classification of Diseases for Oncology (ICD-O), Third ed., WHO, Geneva, 2000.